Flexible and Printed Electronics

PAPER

Flexible ITO-free sky-blue polymer light-emitting diodes and printed polymer solar cells based on AgNW/PI transparent conductive electrode

Xiaolong Yin[1], Jing Wang[1], Alei Liu[1], Wanzhu Cai[1], Lei Ying[2] ⓘ, Xin He[3] ⓘ, Zhenfang Tang[1,4] and Lintao Hou[1,4] ⓘ

1   Guangzhou Key Laboratory of Vacuum Coating Technologies and New Energy Materials, Guangdong Provincial Engineering Technology Research Center of Vacuum Coating Technologies and New Energy Materials, Siyuan Laboratory, Physics Department, Jinan University, Guangzhou 510632, People's Republic of China
2   Institute of Polymer Optoelectronic Materials & Devices, State Key Laboratory of Luminescent Materials & Devices, South China University of Technology, Guangzhou 510640, People's Republic of China
3   School of Applied Physics and Materials, Wuyi University, Jiangmen 529020, Guangdong, People's Republic of China
4   Authors to whom any correspondence should be addressed.

E-mail: ttangzf@jnu.edu.cn and thlt@jnu.edu.cn

Abstract

In this work, transparent and conductive as well as flexible silver nanowire/polyimide (AgNW/PI) composite film with an average figure of merit as high as 111.3, which is the ratio of electronic conductivity to optical conductivity, is produced by a simple peel-off method without any post treatments. When employing the AgNW/PI composite film as the flexible transparent conductive anode in blue polymer light-emitting diodes, the device shows a high external quantum efficiency of 3.42% which is comparable to the rigid indium tin oxide (ITO)-based control device with an efficiency of 3.96%. Moreover, for the flexible printed polymer solar cell (PSCs) with AgNW/PI as the transparent conductive anode, a high power conversion efficiency of 4.01% is achieved, which is also comparable to that of the rigid ITO-based PSC. This work systematically demonstrates that AgNW/PI composite film has a promising prospect for application in all kinds of flexible optoelectronic devices.

1. Introduction

Transparent conductive electrodes (TCEs) play an irreplaceable role in optoelectronic devices, such as light-emitting diodes, solar cells, flat panel displays, and so on [1–4]. Indium tin oxide (ITO) has been widely used as TCE since it has high transmittance (>80%) and low sheet resistance (<20 ohm sq^{-1}). However, with the increasing demand for miniaturized flexible portable and wearable electronic devices, ITO fails to meet the requirement due to its brittleness and nonflexibility [5, 6]. Moreover, high-cost sputtering process and the rarity of indium on earth also limit it widespread usage, attracting people to find more alternatives. In the last few decades, several excellent TCEs have emerged to replace ITO including carbon nanotube [7, 8], graphene [9, 10], conductive polymer [11, 12] and metal nanowires [13–16]. Among them, silver nanowire (AgNW) is regarded as the most promising candidate for ITO because of its high

conductivity and transmittance, good flexibility and easy patternability [17–22]. However, AgNW TCE is still far from commercial use for several crucial drawbacks. For example, in order to enhance the dispersibility of the AgNW, an insulated additive of polyvinylpyrrolidone is usually added into AgNW dispersion, which leads to a high resistance for AgNW films [23, 24]. Although a heating process is adopted to solve this problem, however, the temperature is too high (>200 °C) to be used in plastic substrates [25, 26]. It is reported that some low temperature methods, such as UV light-induced heating [27, 28], microwave sintering [29, 30] and laser radiation [31, 32], were developed to avoid heating, but they are either complicated or expensive to be prepared. Moreover, since thin-film optoelectronic devices are particularly sensitive to the AgNW surface roughness, mechanical pressing with tens of MPa pressure is generally used for obtaining a smooth surface [33, 34]. However, this method is not suitable to rigid substrates due to the

brittleness. Hence, polymer or metallic oxide is used to fill and level up the AgNWs conductive network [35–38]. The most common flexible substrates include poly (vinylalcohol) (PVA) [39], polymethacrylate (PMMA) [40], polydimethylsiloxane (PDMS) [41] and polyimide (PI) [42], etc. Among them, PI has more natural advantages than others such as superb mechanical property and excellent tolerance to heat (above 300 °C) and chemicals, making it become the most promising microelectronics substrate.

Although silver nanowire/polyimide (AgNW/PI) has been reported to be used as TCE in polymer light-emitting diodes (PLEDs) or polymer solar cells (PSCs) [43–48], AgNW/PI used as TCE in both PLEDs and PSCs has never been occurred in previous literatures, making people lack of understanding the universality of AgNW/PI in flexible optoelectronic devices. Moreover, compared to green and red PLEDs, blue PLEDs have a lot of problems to be overcome such as low efficiency and unstable electroluminescence (EL) spectra. Thus the lack of AgNW/PI usage for blue light emitting attracts us to verify the feasibility of application. Furthermore, although there are some reports about AgNW/PI TCE used in PSCs, the active solution is usually prepared by spin-coating, which is not suitable to large-area manufacturing. Thus printing methods, which are suitable to low-cost roll-to-roll fabrication with much little solution wasting, are needed to be employed for active film formation in flexible AgNW/PI-based PSCs.

In this paper, a simple peel-off approach is adopted to obtain AgNW/PI composite TCE, which can not only ameliorate the adhesion of the AgNW to the PI substrate, but also greatly reduce the AgNW surface roughness. Moreover, the AgNW/PI TCE has a high figure of merit (FOM) value of 111.3, which is comparable to the commercial rigid and costly ITO glass substrate. The flexible TCEs of AgNW/PI are used as the substrates for both blue PLEDs and doctor-bladed PSCs, which also work well when compared to control devices based on rigid ITO-coated glass substrates. The results demonstrate that the AgNWs/PI composite TCE is promising for constructing high-precision nanometer scale flexible optoelectronic devices.

2. Experimental section

2.1. Flexible AgNW/PI fabrication process
AgNW suspension (1 wt%) in ethanol was purchased from Zhejiang Kechuang Advanced Materials Co., Ltd. The glass substrates were successively cleaned with acetone, detergent, de-ionized water, and isopropyl alcohol in an ultrasonic bath for 15 min, respectively. Figure 1 shows the detailed schematic diagram of fabrication process of the AgNW/PI composite TCE. AgNW was drop-casted on the clean glass substrate and held to dry in air for 10 min. Then the residual solution was rinsed by de-ionized water and

was heated for 1 min. After that, PI in dimethylformamide (DMAC) solution (14 wt%) was spin-coated on the AgNW film. Immediately, it was cured by a gradient heating process. Finally, the total film was peeled off from the glass substrate. The AgNW conductive network embedded into the PI film was thus produced.

2.2. Flexible blue PLED fabrication on AgNW TCEs
Flexible blue PLEDs were fabricated with AgNW/PI as the TCE. For comparison, the rigid ITO-based PLED was also fabricated. Here, a neutral hole injection layer (HIL) material, HIL-E 100 (Heraeus Group) was applied, which can avoid eroding the AgNW electrode. HIL-E was spin-coated on the AgNW/PI substrate and then annealed at 120 °C for 10 min. Then blue light-emitting polymer poly(fluorine-*co*-dibenzothiophene-*S,S*-dioxide) with triphenylamine substituent (PFSO-T5) in o-xylene solvent (12 mg ml^{-1}) was spin-coated onto it as the emitting layer (EML). Finally, 1.5 nm CsF and 120 nm aluminum (Al) were evaporated in sequence onto the emitting layer under a vacuum of 2×10^{-4} Pa. The effective area of PLEDs is 0.14 cm^2 which is defined by a mask.

2.3. Printed flexible PSCs fabrication on AgNW TCE
Flexible PSCs with an inverted structure were prepared by doctor-blade printing on AgNW/PI composite TCEs. Zinc oxide nanoparticle (ZnONP) dispersed in 2-propanol solvent was purchased from Avantama. ZnONP dispersion solution was spin-coated at 2200 rpm on the AgNW/PI substrate as the electron transport layer (ETL) and annealed at 80 °C for 2 min. The blend of poly(4,8-bis[5-(2-ethylhexyl)thiophen-2-yl]benzo[1,2-b:4,5-b′]dithiophene-2,6-diyl-alt-3-fluoro-2-[(2-ethylhexyl)carbonyl]thieno[3,4-b]thiophene-4,6-diyl) (PTB7-Th) and [6,6]-phenyl-C71-butyric acid methyl ester (PC$_{71}$BM) with the blending ratio of 1:1.5 was dissolved in chlorobenzene (CB) : 1,8-diiodooctane (DIO) (97:3 by volume) solvents for about 20 h at 60 °C. The PTB7-Th:PC$_{71}$BM bulk heterojunction (BHJ) active layer was doctor-bladed on the ZnONP layer. Finally, 10 nm MoO$_3$ and 100 nm Ag were evaporated in sequence under a vacuum of 2×10^{-4} Pa. The effective area of PSCs is 0.14 cm^2 which is defined by a mask. For comparison, rigid ITO-based PSC was also fabricated.

2.4. Characterization
The sheet resistance of AgNW/PI TCE was measured by a four-point probe system. The transmittances of TCEs were recorded using a UV–vis spectrophotometer. Atomic force microscope (AFM) and scanning electron microscope (SEM) were used for analyzing surface morphology and roughness. The performance of blue PLEDs was characterized by Keithley 2400 and 2700 source meters. The electroluminescence (EL) spectrum was recorded by an optics
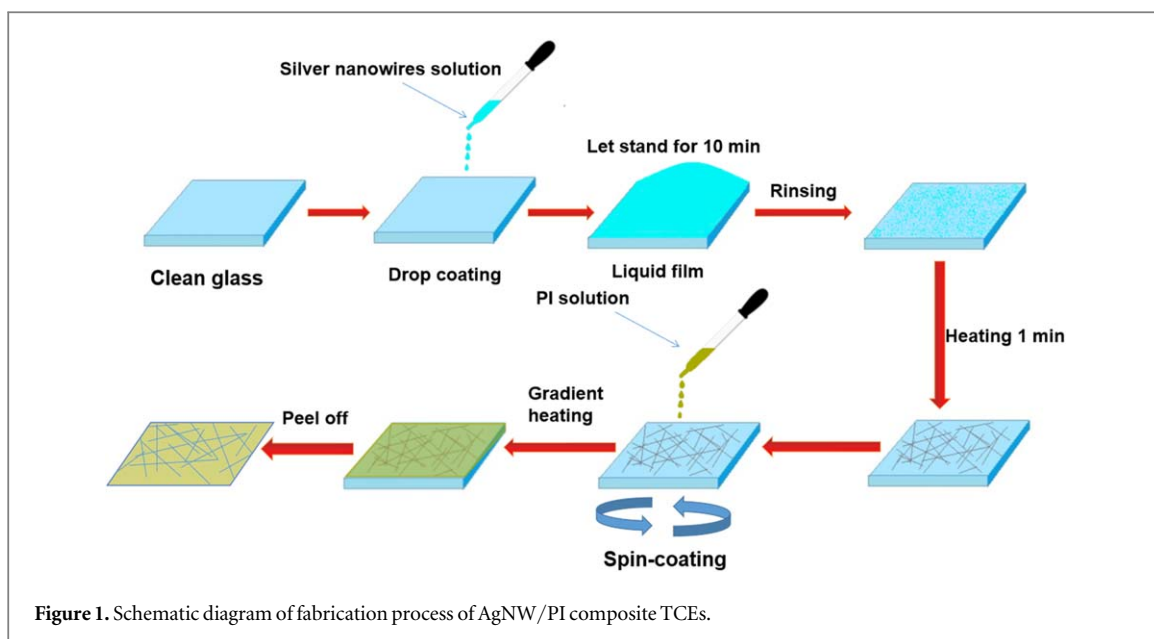
Figure 1. Schematic diagram of fabrication process of AgNW/PI composite TCEs.
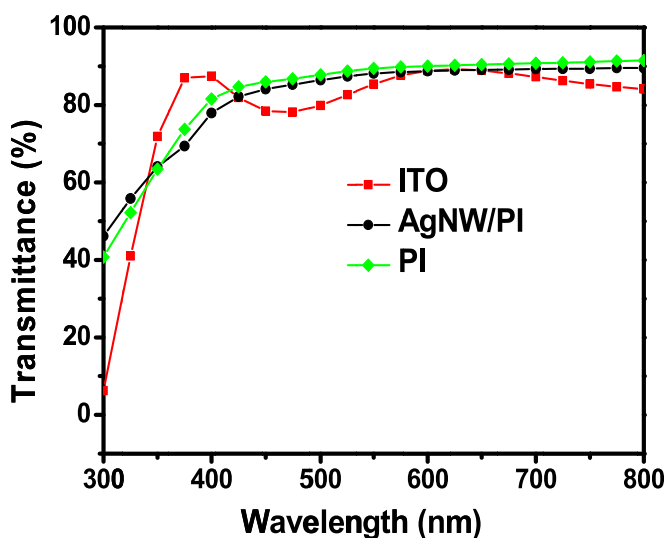

Figure 2. Transmittance spectra of PI, AgNW/PI and ITO/glass.

photometer (USB4000, Ocean Optics). The performance of printed PSCs was characterized by a Keithley 2400 source meter under illumination of AM 1.5G solar simulators with an intensity of 100 mW cm^{-2} (Sun 2000, Abet). Transient photovoltage (TPV) was performed by Paios instrument.

3. Results and discussions

Generally, the transmittance and conductivity show a negative correlation as high optical transmittance means low electrical conductivity in TCEs. The ratio of DC conductivity and optical conductivity (σ_{DC}/σ_{OP}), named as figure of merit (FOM), is popularly used to evaluate the quality of TCEs with different transmittances and sheet resistances. It is related to transmittance (T) and sheet resistance (R_s) which can

be expressed as $T = [1 + (188.5/R_s)(\sigma_{DC}/\sigma_{OP})]^{-2}$. Figure 2 shows the transmittance of pure PI film and AgNW/PI composite film as well as ITO/glass film. It can be seen that the transmittance of AgNW/PI composite film is even a little higher than that of ITO/glass and less influenced by AgNW compared to the pure PI substrate. In our case, the AgNW/PI composite film has an average sheet resistance of 20 Ω sq^{-1} and an average transmittance of 85%, resulting in a high FOM of 111.3, which is comparable to the control ITO/glass film with a FOM of 109.

Besides the FOM, the roughness of TCEs is also a critical parameter for preparing thin film optoelectronic devices. Since the peel-off technology has the advantage that most of AgNWs are embed into the PI layer, an obvious decrease of the roughness of AgNW/PI composite film can be obtained. As shown in figure 3(a), the root mean square roughness (R_q) of
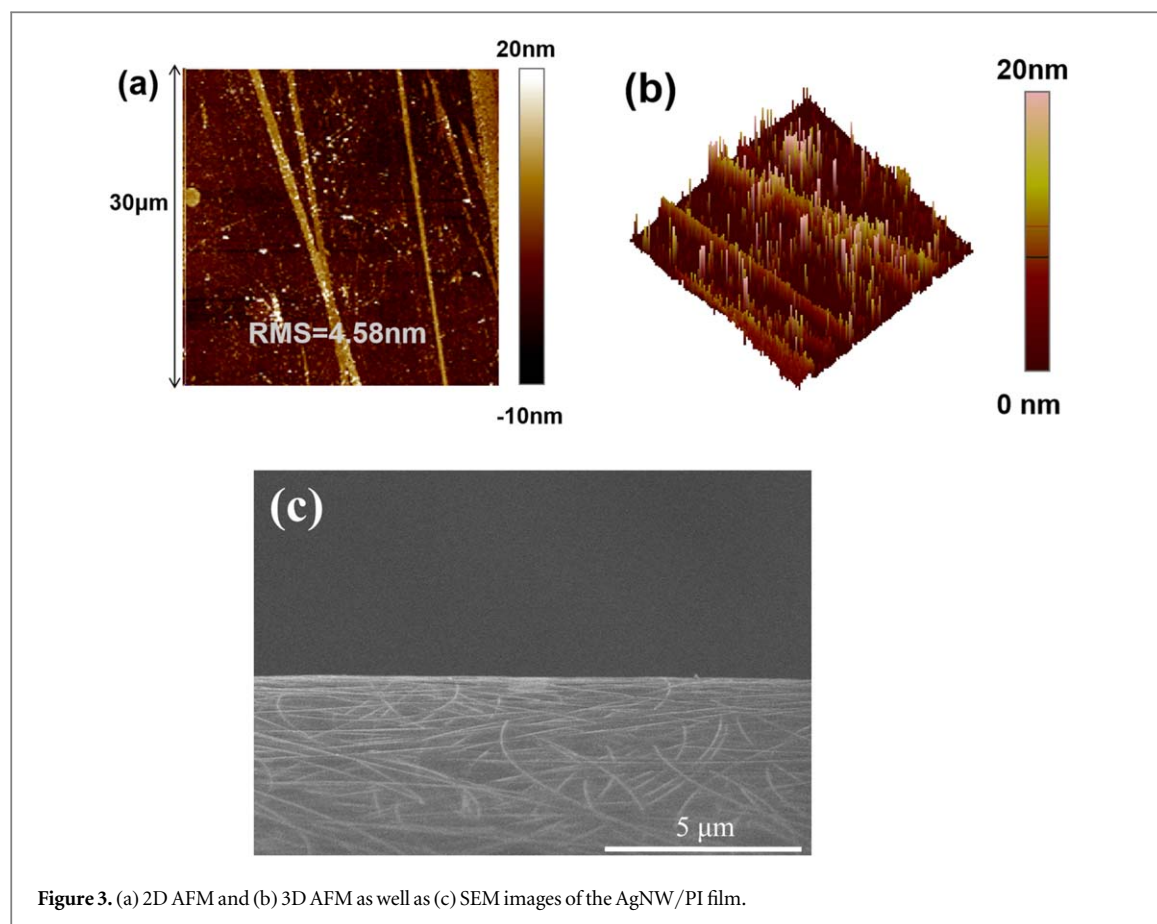
Figure 3. (a) 2D AFM and (b) 3D AFM as well as (c) SEM images of the AgNW/PI film.

Table 1. Detailed optoelectrical performance of flexible AgNW/PI-based and rigid ITO-based blue PLEDs.

TCFs	V_{on}[a](V)	L_{max}(cd m^{-2})	LE_{max}(cd A^{-1})	EQE_{max}(%)	At 1000 cd m^{-2}	
					LE(cd A^{-1})	CIE(*x,y*)
AgNW	4.38	3489	2.74	3.42	2.34	(0.17, 0.24)
ITO	4.19	7542	3.17	3.96	1.53	(0.17, 0.23)

[a] Corresponding to 1 cd m^{-2}.

AgNW/PI composite film displays a low value of 4.58 nm in a large area of $30 \times 30 \ \mu m^2$ with the height between the valley and peak lower than 20 nm (figure 3(b)), which is very advantageous for optoelectronic device fabrication since it can avoid device breakdown and leakage. In addition, it can be seen from SEM image that AgNWs are evenly distributed on the PI surface (figure 3(c)). The scale difference of AgNW in morphologies of AFM and SEM images may come from the mismatch of the used driving force in AFM and the accelerating voltage in SEM [47]. It can be predicted that AgNW/PI is very suitable to be used in flexible optoelectronic devices due to the high FOM and low R_q.

For verifying the application of AgNW/PI in blue PLEDs, the device with the structure of PI/AgNW/HIL-E 100/PFSO-T5/CsF/Al was fabricated. For comparison, traditional ITO-based rigid device with the similar structure was also fabricated. The detailed optoelectrical performances of flexible AgNW/PI-based and rigid ITO-based blue PLEDs are shown in figure 4 and table 1. The two types of blue PLEDs with different TCEs show the close V_{on} of 4.38 V and 4.19 V, respectively. The lower current density of AgNW-based PLEDs than ITO-based PLEDs at low voltage indicates that the flexible AgNW/PI substrate has very small leakage current. This is because that the HIL-E 100 has excellent planarization effect on silver nanowires, resulting in a smoother conductive network. The luminance efficiency (LE) of AgNW/PI-based flexible blue PLED is 2.34 cd A^{-1} at a luminance of 1000 cd m^{-2}, which is 53% higher than the device based on ITO/glass (1.53 cd A^{-1}). The external quantum efficiency (EQE)$_{max}$ of AgNW-based flexible blue PLED is 3.42%, which is comparable with that of rigid ITO-based PLED (3.96%) (figure 4(e)). Figure 4(f) shows the EL spectra of two blue PLEDs with flexible AgNW/PI and rigid ITO/glass electrodes. The EL
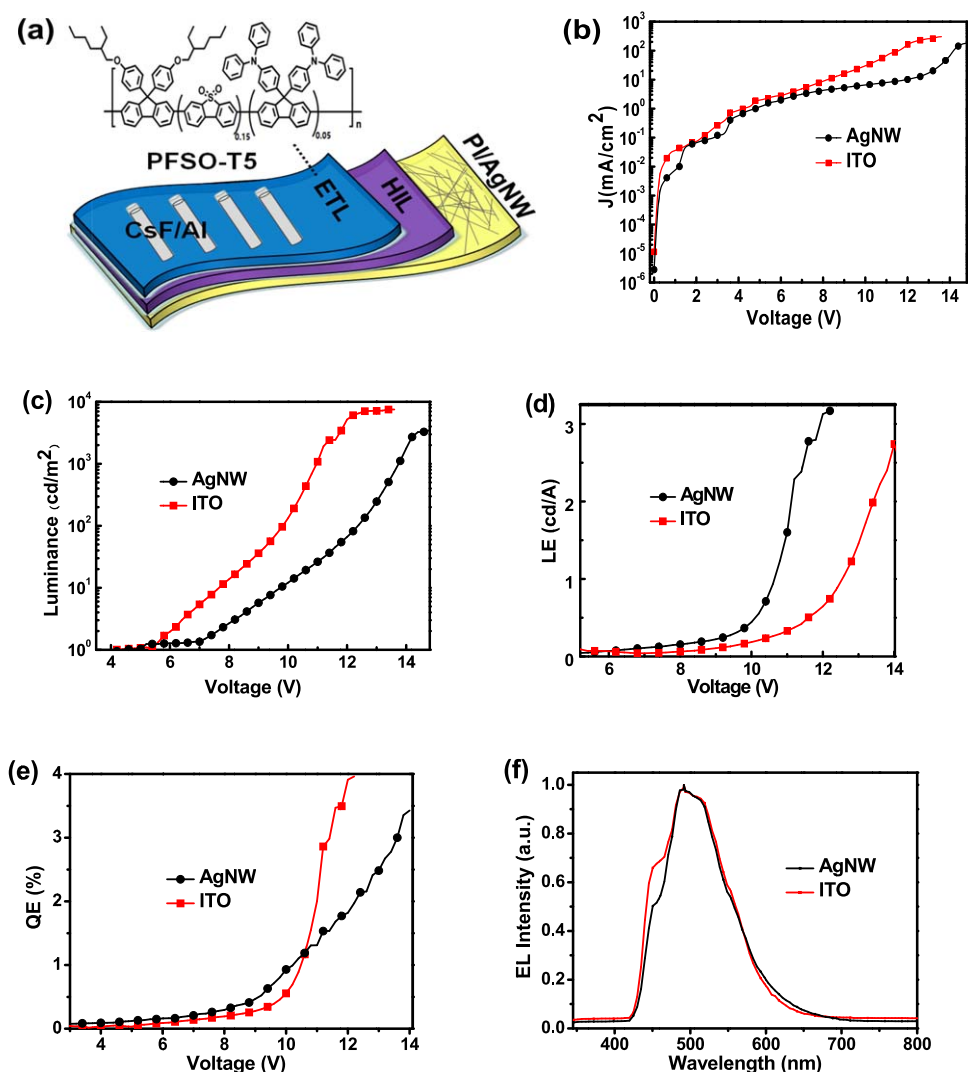
Figure 4. (a) Molecular structure of PFSO-T5 and device structure of flexible blue PLED with AgNW/PI TCE. (b)–(f) *J–V*, *L–V*, *LE–V*, *EQE–V* curves and EL spectra of flexible AgNW/PI-based and rigid ITO-based blue PLEDs.

Table 2. Photovoltaic parameters of printed flexible AgNW/PI-based and rigid ITO-based PSCs under illumination of AM 1.5G (100 mW cm^{-2}).

TCFs	V_{oc}(V)	J_{sc}(mA cm^{-2})	FF(%)	PCE$_{max}$(PCE$_{ave}$)(%)
AgNW	0.75	12.21	43.6	4.01(3.99)
ITO	0.75	16.27	42.2	5.15(5.14)

spectrum of AgNW-based device with CIE (0.17, 0.24) is identical to that of ITO-based device with CIE (0.17, 0.23), indicating the surface plasmon resonance absorption of AgNW in flexible PI substrates is negligible [43].

To prove the universality of flexible AgNW/PI composite film as TCE in other optoelectric devices with printing technology, PSCs with the structure of PI/AgNW/ZnONP/PTB7-th:PC$_{71}$BM/MoO$_3$/Ag were also fabricated by doctor-blade printing. As shown in figure 5 and table 2, the printed flexible AgNW-based device and printed rigid ITO-based device show the same V_{oc} and similar fill factor (FF),

whereas the a low J_{sc} is achieved for AgNW/PI-based PSC compared to ITO-based PSC, resulting in a comparably low power conversion efficiency (PCE) of 4.01%. The different J_{sc} is mainly determined by morphology defects formed in doctor-bladed active layers. Moreover, the EQE spectra of two kinds of printed PSCs correspond well to the measured J_{sc} values. In our case, it seems that a well-printed active layer is more difficult to be achieved for flexible AgNW/PI than for rigid ITO/glass, because AgNW/PI was bent during the doctor-blade process. Thus the PI film thickness should be further increased for eliminating the bending effect during the doctor-blade
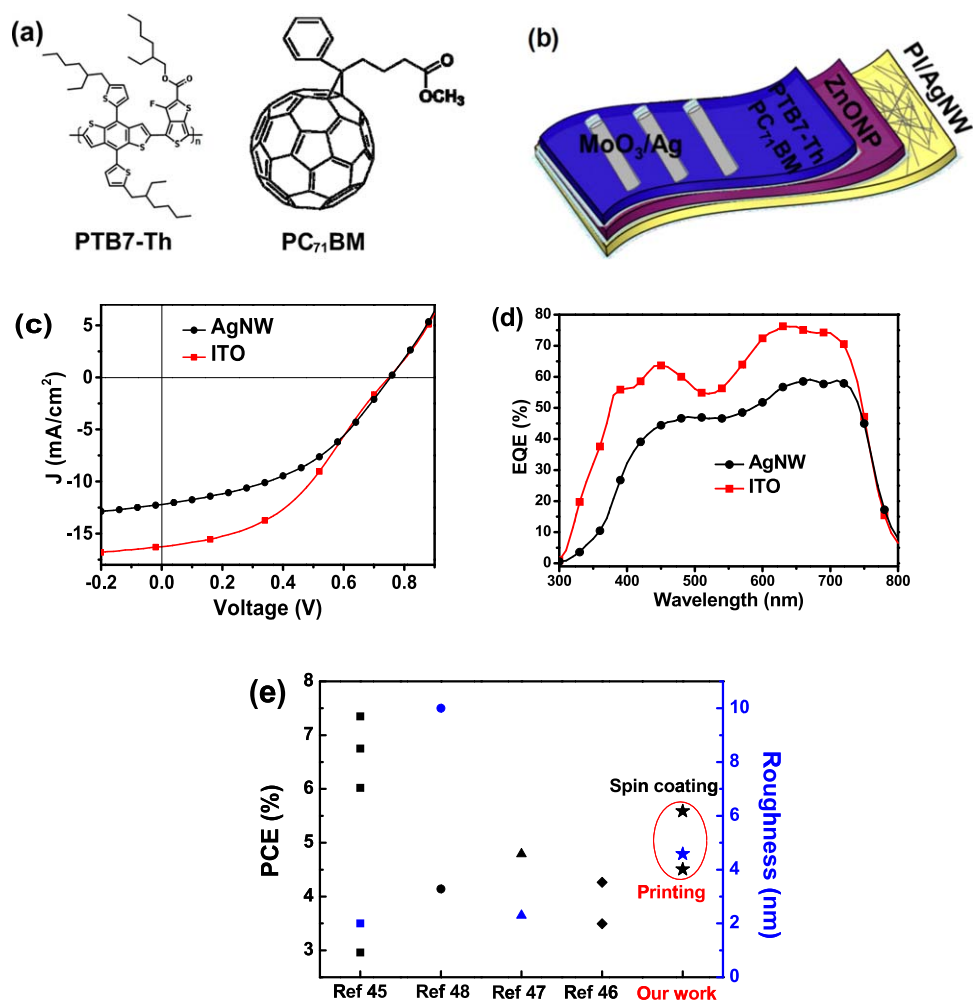
Figure 5. (a) Molecular structures of PTB7-Th donor and PC$_{71}$BM acceptor. (b) Device structure of printed flexible PSCs. (c) *J–V* curves and (d) EQE spectra of printed flexible AgNW-based and printed rigid ITO-based PSCs. (e) Comparison of the performance with previous reported spin-coated fullerene PSCs with AgNW/PI TCEs.
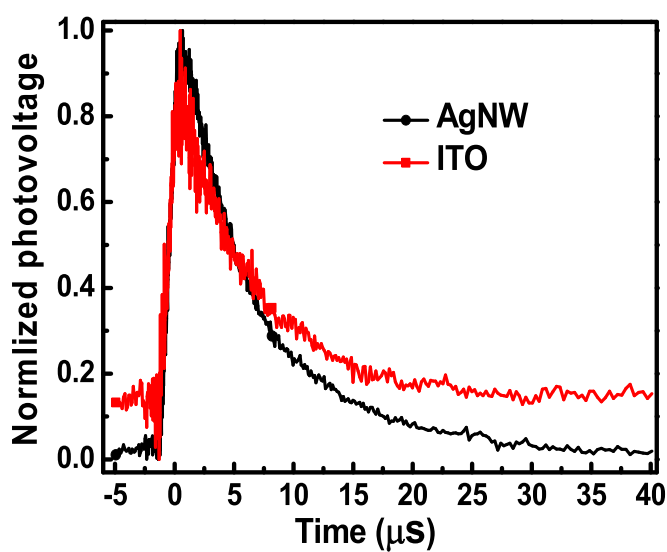

Figure 6. TPV of printed flexible AgNW-based and rigid ITO-based devices measured under 72 mW cm^{-2} and V_{oc} conditions.

printing process. As presented in figure 5(e), the PCE of the spin-coated PSCs with AgNW/PI TCEs is comparable to previous spin-coated fullerene-based PSCs with AgNW/PI TCEs reported to date. More importantly, the PCE of the doctor-blade printed PSCs with AgNW/PI TCEs in this work is even higher than some representative spin-coated fullerene PSCs with AgNW/PI TCEs. In addition, the roughness value of AgNW/PI TCEs is comparable to the reported ones.

To further understand the reason of different performance between two types of printed PSCs, TPV measurement was performed to probe charge transport and collection characteristics in device. Figure 6 shows the TPV results of printed flexible AgNW-based and rigid ITO-based PSCs. The extracted carrier lifetime is 6.17 μs for printed AgNW-based device, whereas it is 6.36 μs for printed ITO-based device. Generally, a short carrier lifetime is closely related to an increased bimolecular recombination. In this case, since the nongeminate recombination in printed rigid ITO-based PSCs is a bit weaker than printed flexible AgNW-based solar cells, a higher J_{sc} in a rigid device is correspondingly produced.

4. Conclusions

In conclusion, we demonstrate a simple peel-off method to fabricate the AgNW/PI composite films without any post-treatments. A high FOM value of 111.3 is achieved for AgNW/PI TCE, which is comparable to that of ITO. Moreover, due to the flowability of PI, most of the AgNWs are enwrapped inside it, resulting in a very smooth surface with R_q of only 4.58 nm. The composite TCEs can be successfully utilized in flexible blue PLEDs and printed PSCs, respectively, with the comparable device performance to ITO-based ones. Based on the above results, it is believed that the AgNW/PI composite film is a promising TCE candidate for next-generation flexible optoelectronic devices.

Acknowledgments

ORCID iDs

Lei Ying https://orcid.org/0000-0003-1137-2355
Xin He https://orcid.org/0000-0002-1018-3512
Lintao Hou https://orcid.org/0000-0002-4358-3862

References

[1] Liu A *et al* 2019 Manipulate micrometer surface and nanometer bulk phase separation structures in the active layer of organic solar cells via synergy of ultrasonic and high-pressure gas spraying *ACS Appl. Mater. Interfaces* **11** 10777–84

[2] Jurewicz I, Fahimi A, Lyons P E, Smith R J, Cann M, Large M L, Tian M, Coleman J N and Dalton A B 2014 Insulator-conductor type transitions in graphene-modified silver nanowire networks: a route to inexpensive transparent conductors *Adv. Funct. Mater.* **24** 7580–7

[3] Sun J *et al* 2016 Direct chemical-vapor-deposition-fabricated, large-scale graphene glass with high carrier mobility and uniformity for touch panel applications *ACS Nano* **10** 11136–44

[4] Lan W *et al* 2017 Ultraflexible transparent film heater made of Ag nanowire/PVA composite for rapid-response thermotherapy pads *ACS Appl. Mater. Interfaces* **9** 6644–51

[5] Galagan Y, J M Rubingh J-E, Andriessen R, Fan C-C, W M Blom P, C Veenstra S and M Kroon J 2011 ITO-free flexible organic solar cells with printed current collecting grids *Sol. Energy Mater. Sol. Cells* **95** 1339–43

[6] Wang H, Li K, Tao Y, Li J, Li Y, Gao L L, Jin G Y and Duan Y 2017 Smooth ZnO:Al-AgNWs composite electrode for flexible organic light-emitting device *Nanoscale Res. Lett.* **12** 77

[7] Chien Y M, Lefevre F, Shiah I and Izquierdo R 2010 A solution processed top emission OLED with transparent carbon nanotube electrodes *Nanotechnology* **21** 134020

[8] Balashangar K, Paranthaman S, Thanihaichelvan M, Amalraj P A, Velauthapillai D and Ravirajan P 2018 Multi-walled carbon nanotube incorporated nanoporous titanium dioxide electrodes for hybrid polymer solar cells *Mater. Lett.* **219** 265–8

[9] Yang S-Y, Park J and Kim Y-S 2015 Polyelectrolyte/graphene oxide barrier film for flexible OLED *J. Nanosci. Nanotechnol.* **15** 7795–9

[10] Wu J, Becerril H A, Bao Z, Liu Z, Chen Y and Peumans P 2008 Organic solar cells with solution-processed graphene transparent electrodes *Appl. Phys. Lett.* **92** 263302

[11] Yousefi M H, Fallahzadeh A, Saghaei J and Davoudi Darareh M 2016 Fabrication of flexible ITO-free OLED using vapor-treated PEDOT:PSS thin film as anode *J. Display Technol.* **12** 1647–51

[12] Na S-I, Kim S-S, Jo J and Kim D-Y 2008 Efficient and flexible ITO-free organic solar cells using highly conductive polymer anodes *Adv. Mater.* **20** 4061–7

[13] Song M *et al* 2013 Highly efficient and bendable organic solar cells with solution-processed silver nanowire electrodes *Adv. Funct. Mater.* **23** 4177–84

[14] Stewart I E, Rathmell A R, Yan L, Ye S, Flowers P F, You W and Wiley B J 2014 Solution-processed copper-nickel nanowire anodes for organic solar cells *Nanoscale* **6** 5980–8

[15] Lian L, Wang H, Dong D and He G 2018 Highly robust and ultrasmooth copper nanowire electrode by one-step coating for organic light-emitting diodes *J. Mater. Chem. C* **6** 9158–65

[16] Lian L, Xi X, Dong D and He G 2018 Highly conductive silver nanowire transparent electrode by selective welding for organic light emitting diode *Org. Electron.* **60** 9–15

[17] Joo Y, Byun J, Seong N, Ha J, Kim H, Kim S, Kim T, Im H, Kim D and Hong Y 2015 Silver nanowire-embedded PDMS with a multiscale structure for a highly sensitive and robust flexible pressure sensor *Nanoscale* **7** 6208–15

[18] Bade S G *et al* 2016 Fully printed halide perovskite light-emitting diodes with silver nanowire electrodes *ACS Nano* **10** 1795–801

[19] Lee J *et al* 2017 A dual-scale metal nanowire network transparent conductor for highly efficient and flexible organic light emitting diodes *Nanoscale* **9** 1978–85

[20] Leem D S, Edwards A, Faist M, Nelson J, Bradley D D and de Mello J C 2011 Efficient organic solar cells with solution-processed silver nanowire electrodes *Adv. Mater.* **23** 4371–5

[21] Wang B-Y, Lee E-S, Oh Y-J and Kang H W 2017 A silver nanowire mesh overcoated protection layer with graphene

oxide as a transparent electrode for flexible organic solar cells *RSC Adv.* **7** 52914–22

[22] Li D, Lai W Y, Zhang Y Z and Huang W 2018 Printable transparent conductive films for flexible electronics *Adv. Mater.* **30** 1704738

[23] Lee J-Y, Stephen T C, Yi C and Peter P 2008 Solution-processed metal nanowire mesh transparent electrodes *Nano Lett.* **8** 689–92

[24] Langley D P, Lagrange M, Giusti G, Jimenez C, Brechet Y, Nguyen N D and Bellet D 2014 Metallic nanowire networks: effects of thermal annealing on electrical resistance *Nanoscale* **6** 13535–43

[25] Jia Y, Chen C, Jia D, Li S, Ji S and Ye C 2016 Silver nanowire transparent conductive films with high uniformity fabricated via a dynamic heating method *ACS Appl. Mater. Interfaces* **8** 9865–71

[26] Tang Q, Shen H, Yao H, Jiang Y, Zheng C and Gao K 2017 Preparation of silver nanowire/AZO composite film as a transparent conductive material *Ceram. Int.* **43** 1106–13

[27] Chung W-H, Park S-H, Joo S-J and Kim H-S 2018 UV-assisted flash light welding process to fabricate silver nanowire/graphene on a PET substrate for transparent electrodes *Nano Res.* **11** 2190–203

[28] Belenkova T L, Rimmerman D, Mentovich E, Gilon H, Hendler N, Richter S and Markovich G 2012 UV induced formation of transparent Au–Ag nanowire mesh film for repairable OLED devices *J. Mater. Chem.* **22** 24042

[29] Gao J *et al* 2013 Transparent nanowire network electrode for textured semiconductors *Small* **9** 733–7

[30] Perelaer J, de Gans B J and Schubert U S 2006 Ink-jet printing and microwave sintering of conductive silver tracks *Adv. Mater.* **18** 2101–4

[31] Lin L, Huang H, Sivayoganathan M, Liu L, Zou G, Duley W W and Zhou Y 2015 Assembly of silver nanoparticles on nanowires into ordered nanostructures with femtosecond laser radiation *Appl. Opt.* **54** 2524–31

[32] Park J-Y, Seungpyo H, Jin J and Kim H-K 2017 Blue laser annealing of Ag nanowire electrodes for flexible thin film heaters *ECS J. Solid State Sci. Technol.* **6** 746–51

[33] Tokuno T, Nogi M, Karakawa M, Jiu J, Nge T T, Aso Y and Suganuma K 2011 Fabrication of silver nanowire transparent electrodes at room temperature *Nano Res.* **4** 1215–22

[34] Hu L, Kim H, Lee J, Peumans P and Cui Y 2010 Scalable coating and properties of transparent, flexible, silver nanowire electrodes *ACS Nano* **4** 2955–63

[35] Gaynor W, Burkhard G F, McGehee M D and Peumans P 2011 Smooth nanowire/polymer composite transparent electrodes *Adv. Mater.* **23** 2905–10

[36] Duan S, Zhang L, Wang Z and Li C 2015 One-step rod coating of high-performance silver nanowire–PEDOT:PSS flexible

electrodes with enhanced adhesion after sulfuric acid post-treatment *RSC Adv.* **5** 95280–6

[37] Song M, Park J H, Kim C S, Kim D-H, Kang Y-C, Jin S-H, Jin W-Y and Kang J-W 2014 Highly flexible and transparent conducting silver nanowire/ZnO composite film for organic solar cells *Nano Res.* **7** 1370–9

[38] Chen D, Liang J, Liu C, Saldanha G, Zhao F, Tong K, Liu J and Pei Q 2015 Thermally stable silver nanowire-polyimide transparent electrode based on atomic layer deposition of zinc oxide on silver nanowires *Adv. Funct. Mater.* **25** 7512–20

[39] Lian L, Dong D, Feng D and He G 2017 Low roughness silver nanowire flexible transparent electrode by low temperature solution-processing for organic light emitting diodes *Org. Electron.* **49** 9–18

[40] Choo D C, Lee J G and Kim T W 2015 Transparent conducting silver-nanowire-embedded poly(methyl methacrylate) nanocomposite films formed by using a transfer method *J. Nanosci. Nanotechnol.* **15** 7598–601

[41] Lee J-Y, Shin D and Park J 2016 Fabrication of silver nanowire-based stretchable electrodes using spray coating *Thin Solid Films* **608** 34–43

[42] Spechler J A, Koh T-W, Herb J T, Rand B P and Arnold C B 2015 A transparent, smooth, thermally robust, conductive polyimide for flexible electronics *Adv. Funct. Mater.* **25** 7428–34

[43] Lee K M, Fardel R, Zhao L, Arnold C B and Rand B P 2017 Enhanced outcoupling in flexible organic light-emitting diodes on scattering polyimide substrates *Org. Electron.* **51** 471–6

[44] Kim D W, Han J W, Lim K T and Kim Y H 2017 Highly enhanced light-outcoupling efficiency in ITO-free organic light-emitting diodes using surface nanostructure embedded high-refractive index polymers *ACS Appl. Mater. Interfaces* **10** 985–91

[45] Kim Y *et al* 2015 Inverted layer-by-layer fabrication of an ultraflexible and transparent Ag nanowire/conductive polymer composite electrode for use in high-performance organic solar cells *Adv. Funct. Mater.* **25** 4580–9

[46] He X, Duan F, Liu J, Lan Q, Wu J, Yang C, Yang W, Zeng Q and Wang H 2017 Transparent electrode based on silver nanowires and polyimide for film heater and flexible solar cell *Materials* **10** 1362

[47] Guo X, Liu X, Luo J, Gan Z, Meng Z and Zhang N 2015 Silver nanowire/polyimide composite transparent electrodes for reliable flexible polymer solar cells operating at high and ultra-low temperature *RSC Adv.* **5** 24953–9

[48] Yu Z, Li L, Zhang Q, Hu W and Pei Q 2011 Silver nanowire-polymer composite electrodes for efficient polymer solar cells *Adv. Mater.* **23** 4453–7